A new method for automatic marking epileptic spike-wave discharges in local field potential signals

Sofia A. Startceva[ab], Annika Lüttjohann[cd], Ilya V. Sysoev[a], Gilles van Luijtelaar[c]

[a]Saratov State University, Department of Nano- and Bio-medical technologies, Astrakhanskaya street, 83, Saratov, Russia;
[b]Tampere University of Technology, Department of Signal Processing, Korkeakoulunkatu 1, FI-33720 Tampere, Finland;
[c]Radboud University Nijmegen, Donders Centre for Cognition, Nijmegen, The Netherlands;
[d]University of Münster, Institute of Physiology I, Robert-Koch-Str. 27a, 48149 Münster, Germany

ABSTRACT

This work proposes a new method for automatic marking epileptic spike-wave discharges in local field potential (LFP) signals. The method is based on empirical modelling using radial basis functions to approximate dependency of a further state on the current one. Number and type of radial basis functions used are adjusted to data based on statistical criteria. Due to this the method needs only a few manual efforts for its application to new data. The time resolution of the method is close to the sampling interval of the original data, and real time detection is possible. Detection accuracy of the proposed approach is validated analysing the LFP signals obtained using WAG/Rij rats.

Keywords: local field potentials, epilepsy, signal processing, radial-basis functions

1. INTRODUCTION

Epilepsy is a complex physiological neurological disorder of recurrent seizures with an estimated prevalence in Europe of 4.3–7.8 per 1000. Regardless of the original brain insult, neocortical epileptic focal sites show remarkable similarity in electrophysiological pattern of localized, abnormal electrical discharges that can become rhythmic and propagate to wider brain regions initiating clinical seizures as a result of anomalous phase synchronisation in ensembles of neurons.[1–3] As a concept in neurobiology, local synchronisation is phase-phase and phase-amplitude synchronisation between several populations of neurons. Synchronised activity in large neuronal ensembles is considered as a major mechanism triggering macro-oscillations in brain function called brain rhythms. In general, rhythms are known to contribute and alter information propagation and neural communication. However, excessive local synchronisation in neuronal networks can induce disabling disorders such as epileptic seizures, tremor in the Parkinson disease, and abnormal higher cortical functions.[4]

Absence seizures are most frequently observed in 4–12 year old children (childhood absence epilepsy) and in adolescents with juvenile absence epilepsy. Inherent to these seizures are a high reoccurrence and their short (5–30 s) duration, often accompanied by the absence of consciousness. These seizures can be detected in an electroencephalogram (EEG) as a specific spike-wave pattern at a frequency about 3 Hz.[5,6] The seizures occurring in young children have been modelled using a genetic absence model, such as rats of the WAG/Rij strain, a well validated genetic absence model,[7] to record local field potentials, also in deep cerebral structures.

To distinguish ictal and interictal periods one routinely uses a visual marking method,[8] yet, analysis of EEG signals may involve more complex mathematical methodologies. It has been noticed that the recognition algorithms can employ several approaches based on (i) statistical; (ii) mathematical; and (iii) neural network analysis.[9] A statistical approach assumes that the potential variations in the neural network are stationary stochastic events in time, additive to a non-stationary process. This makes detection of unpredictable events

Further author information: (Send correspondence to Ilya V. Sysoev)
Ilya V. Sysoev: E-mail: ivssci@gmail.com

Saratov Fall Meeting 2014: Optical Technologies in Biophysics and Medicine XVI; Laser Physics and Photonics XVI; and Computational Biophysics, E. A. Genina, V. L. Derbov, K. V. Larin, D. E. Postnov, V. V. Tuchin, Eds., Proc. of SPIE Vol. 9448, 94481R · © 2015 SPIE · CCC code: 1605-7422/15/$18 · doi: 10.1117/12.2179017

problematic. The second group mostly includes a time-frequency analysis with the concept of wavelets being explored to treat physiological signals.[10,11] As a recent example of the third approach, we note an application of a neural network training algorithm for spike-wave detection based on an intracranial local field potential (LPF) recording.[12]

In this work we analyse experimental LFP data taken from WAG/Rij rats. First, we give the theoretical basis of our automatic marking method, present the developed algorithm and verify the method's robustness by applying the method to noisy oscillatory model signals. Second, we describe the experimental data and process the data with our developed method. Finally, we discuss the results obtained.

2. METHODS

In the frames of the proposed method we consider the observed LFP signals as realisations of a complex dynamical system (or stochastic system, where noise does not introduce any new principle features and only affects the horizon of predictability). For such signals empirical (i. e. based on properties of these signals themselves) predictive (or autoregressive) models (i. e. of type (1)) can be constructed.[13]

$$x'_{n+\tau} = f\left(x_n, x_{n-l}, \ldots, x_{n-(D-1)l}\right), \tag{1}$$

where f is an approximating function, x_n is a current measured state, while x'_n is a current predicted state (mean squared difference between x_n and x'_n is an approximation error), D is a model dimension (the number of data points used for prediction), l is a lag that is a distance between the used data points, and τ is the prediction time.

The main idea is that the prediction error of the model, constructed from a fragment of signal considered as an absence seizure, is significantly smaller for all seizures than for other, non-absence fragments of series. However, first application of such a straightforward idea showed that it is not sufficient due to the fact that a real LFP signal consists of not only absences and normal activity (that also has different stages, e. g. activity during sleeping period differs from the activity during awake state), but also of artefacts and abnormal but not absence patterns. Therefore, the method is based on two models: one for the absences and the other for an awake normal state (baseline activity). The awake state was chosen due to the fact that the transition from passive wakefulness to SWD occurs most often.

2.1 Radial basis functions

It has been mentioned[13] that to get a good enough predictive model one has to take into account all the individual properties of the considered signals. Since absence seizures seem to be highly nonlinear phenomena, radial basis functions[14] were chosen for computing the approximation function f.

An approximation function is normally a result of a finite quantity of combinations among the radially symmetric basis functions defined as $\phi(\|\cdot\|)$, were $\|\cdot\|$ is the Euclidean norm. Radially symmetric functions are rotationally invariant, and the value $f(x)$ depends only on the Euclidean distance between the parameter and the zero point. Radial basis function spaces are spanned by translates $\phi(\|\cdot - o\|)$, where $o \subset x$ are chosen centres. In general, its function is given by (2), where λ_k are real coefficients, $\phi(\|\cdot - o\|) = \phi(r)$ is the radial basis function, k is a centre number.[14–16] In this work coefficients λ_k are computed via the least squares method.

$$f(x) = \sum_{k=1}^{K} \lambda_k \phi(\|x - o_k\|) \tag{2}$$

In the approximation algorithm we tested radial functions of three types, namely, the flat splines $\phi(r) = r^2 \log r$, the cubic splines $\phi(r) = r^3$, and the Gaussian splines $\phi(r) = e^{-\alpha r^2}$, were α is a positive parameter (Fig. 1).

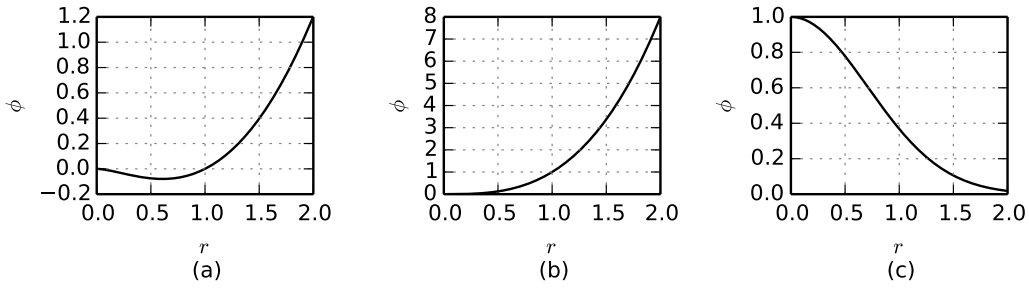

Figure 1. Different types of radial basis functions: (a) — flat splines, (b) — cubic splines, (c) — Gaussian splines.

2.2 Algorithm description

Success in empirical modelling is critically dependent on a right choice of the parameters. First, let us to classify the approximation parameters in groups.

1. *The parameters of embedding*, i.e., the parameters identifying way to obtain state vector $(x_n, x_{n-l}, \ldots, x_{n-(D-1)l})$, in our case they are dimension D and lag l.
2. *The parameters of basis functions*: a type of basis functions, their number K, and their individual properties, in our case — position of nodes.
3. *The predictive parameters*. Here are prediction length τ and threshold values of approximation error that indicate maximum acceptable error for baseline and seizure state, respectively.

The dimension D of the vector of state employed in the calculations varied from 2 to 8 as the accuracy of the model deteriorated at the larger values of D. Given that the global minimum can not be reached algorithmically, and its average error in approximation narrows as the dimensionality of the vector of state increases, and a number of the local minima increases, the probability to get into the global minima of the average error of the approximation vanishes. We used all the three types of the radial basis functions in the calculations. The average error was calculated as (3)

$$\varepsilon^2 = \frac{1}{N_{\text{eff}} - K} \sum_{i=1}^{N} (x'_i - x_i)^2 \Bigg/ \sigma_x^2, \tag{3}$$

were $N_{\text{eff}} = N - (D-1)l - \tau$ is effective length of time series, σ_x^2 is an empirical variance of the measured signal. The prediction time τ was chosen to be 1 for the purpose of better time resolution.

The choice of the nodes, which are used to translate the state vectors, is an important step in construction of the model with the use of radial basis functions. In this work we choose the node positions using the method of K-means, a well known algorithm of clustering.[17] Since results of K-means vary depending on initial guesses for centres of clusters in D dimensional phase space, we performed 1000 attempts of model construction with different random initial conditions, choosing the one, that gives the minimal error ε^2.

Next, we verify sufficiency of the obtained model. Increasing number of the radial basis functions may lead to underestimation of coefficients, notably in noisy systems. To optimize the set of the basis functions, the Schwartz's criterion (also known as Bayesian information criterion) may be employed.[18,19] In the work we use the modified Schwartz criterion (4), which allows to penalty the dimensionality of the vector of state as well.

$$\tilde{S} = \frac{N_{\text{eff}}}{2} \ln \varepsilon^2 + \frac{K \cdot D}{2} \ln \frac{N_{\text{eff}}}{2}, \tag{4}$$

We also analysed model residuals $\xi_n = x_n - x'_n$. The obtained model is adequate if all the residuals do not contain useful information about a signal. The residuals obey two rules:

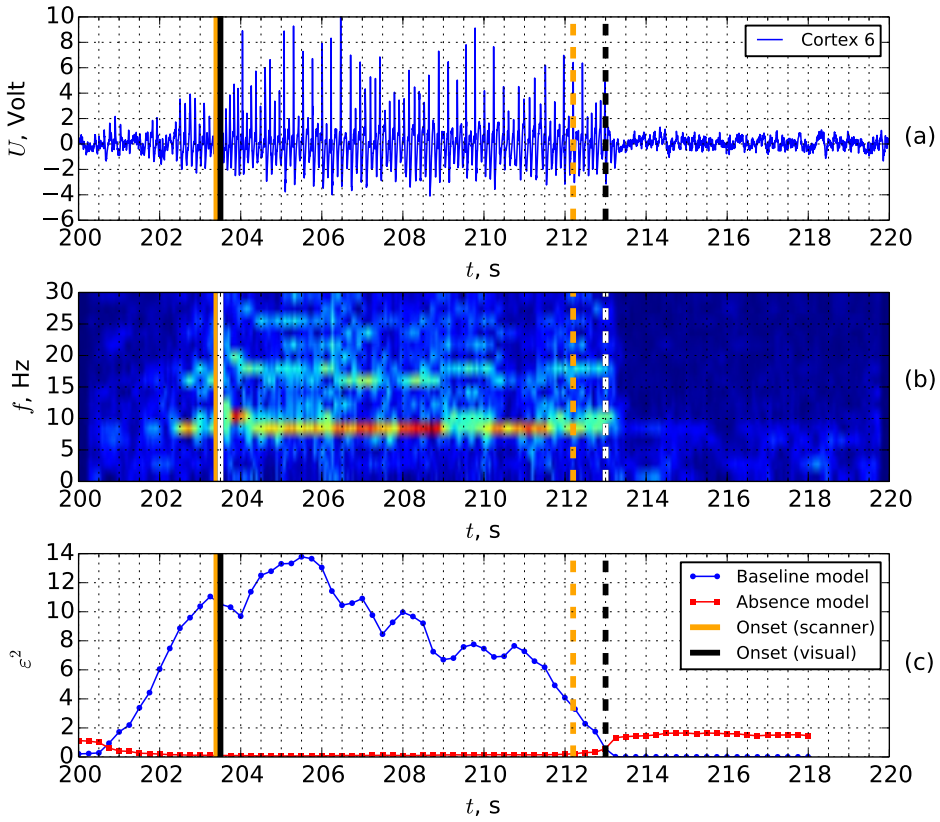

Figure 2. A fragment of the cortical layer 6 time series with an absence seizure (a), its Fourier analysis in sliding window (b), and RBF-model based marking (c). The RBF-based marking is pictured in orange, visual marking is black and white.

1. The normal distribution if noise is not specified to follow any other law.
2. Statistical independence.

To test ξ_n for normality the Kolmogorov-Smirnov test with empirical estimation of mean and variance was used. Since examining the arbitrary statistical interdependence seems to be impossible, only linear interdependence (i. e. correlation) was examined. The above criteria are minimal necessary, but may be not sufficient.

Finally, we applied the verified model to the studied LFP signal in a sliding window, where the window width was chosen empirically to be short enough to include only one signal type per window in most of the cases, and long enough to contain sufficient information about the signal type features. The smaller the average approximation error ε^2, the more the windowed part of the LFP signal resembles the modelled signal. The window shift time should be several times smaller then the window width, so that changes in the signal type can be detected more accurately. Two filters for ε^2 were set: a low-pass filter for a seizure model and a band-pass filter for a baseline model. Both models were applied to predict series in τ points further in a large time interval. When the seizure model error was low enough while the baseline model error was in the set interval of the band-pass filter, the seizure onset marker was set. If the onset marker was set, and the seizure model error surpassed its threshold, or baseline model error became too small or too big, the seizure offset marker was set. A baseline signal model is crucial for the reliability of the method, since a seizure model often suits artefacts as well as absence seizures. In contrast, a baseline signal model is able to differ between seizures, baseline activity and artefacts, though not as precise as when combined with a seizure signal model. For brevity, the described processing can be denoted as the *RBF-model based marking*. The principle of applying the method to experimental data is depicted in Fig. 2.

3. EXPERIMENTAL DATA PROCESSING

3.1 Data description

Data were obtained from a previously used and published data set,[20] in which male WAG/Rij rats, 6 to 9 month of age were used as experimental subjects. The experiment was approved by the Ethical Committee on Animal Experimentation of Radboud University Nijmegen (RU-DEC). LPFs were recorded with a self-constructed electrode system for multi-site EEG recording at specified and verified brain locations. Stainless steel electrodes insulated with poliamide, diameter: $127\mu m$ were fixated in a Teflon block, which contained small holes located at the relative A/P & M/L coordinates of the multiple electrode target structures as determined by the rat brain atlas of Paxinos and Watson.[21] Electrode wires including those from reference and ground were glued to the Teflon-block and fixed at the top-site to a connector pin which was entered into an electrode pedestal suitable for the connection to a multi-lead electrode cable, that was connected to a swivel allowing long term recording in freely moving and well adapted rats. The LFP signals were amplified with a physiological amplifier (TD 90087, Radboud University Nijmegen, Electronic Research Group), filtered by a band pass filter with cut-off points at 1(HP) and 100(LP) and a $50Hz$ Notch filter, and digitalized with a constant sample rate of $2048Hz$ by WINDAQ-recording-system (DATAQ-Instruments). Each rat was recorded for a period of 4 hours during the dark phase. In this work, records from cahnnels 5 (Posterior thalamus), 9 (Cortical layer 5) and 10 (Cortical layer 6) from 6 rats were used.

3.2 Results

3.2.1 Optimal parameters selection

The optimal values of K and D were found separately for each rat considered. To perform this, models for 6 SWD samples and 6 baseline samples per rat were built with parameters $K \in [2; 15]$ and $D \in [2; 8]$. This was done for all three different types of RBFs. As a result, $K = 2$ and $D = 5$ with cubic splines RBFs were chosen for absence seizure model, while $D = 5$, $K = 10$ and the Gaussian RBFs were got for the models of baseline activity.

The optimal parameters selection took several steps. First, approximation error ε^2 must be computed for empirically chosen state vector of dimension D ($2 \leqslant D \leqslant 8$), type and amount of RBF centres, and the modified Bayesian information criterion ($\tilde{S}$) must be applied. Considering that $\tilde{S}$ has its minimum at $K = K_{\tilde{S}}$ (so there is an optimal amount of centres). However, in the case of an autoregression RBF-modelling, the $\tilde{S}$ minimum does not correspond to the optimal centres amount K_{best}. This can be explained taking into account a relatively high noise level of biological signals, and therefore a large approximation error ε^2 (12%) may be allowed. The next step of optimizing parameters is processing LFP signal using models with $D = D_{best}$, K varies, and $K = K_{best}$, D varies, choosing the best one on each iteration. The best model is a model that differs pertaining to signal type changes (baseline activity, seizure, artefact) in the most pronounced way (the approximation error ε^2 proportions are the most contrast).

The fact that for all the 6 studied rats the same optimal parameters from their LFP signals were received is a consequence of the fact that the approximation error ε^2 variation between average models of different rats sample models is not significantly larger than the rats sample model of an individual rat (Fig. 2). This implies that the model parameters choosing step can be omitted in the future for new data. The only model adjustment we need is choosing clear enough fragments of seizure and baseline and setting low-pass filter and band-pass filter boundaries for absence seizure model and baseline signal model respectively.

3.2.2 Data processing: Evaluation

12300 seconds of LFP obtained from one WAG/Rij rat (cortical layer 6, cortical layer 5 and posterior thalamic nucleus (TN) channels) were analysed using two different methods: visually with the aid of a Fourier analysis, and by means of the developed algorithm.

The LFP was processed with two sample models: one of an absence seizure and one of a baseline signal. Each model was constructed from 2 second intervals of baseline/absence activity of the same rat respectively. Three different sample model pairs were applied to the data in a sliding window with the window shift time of 0.25 s.

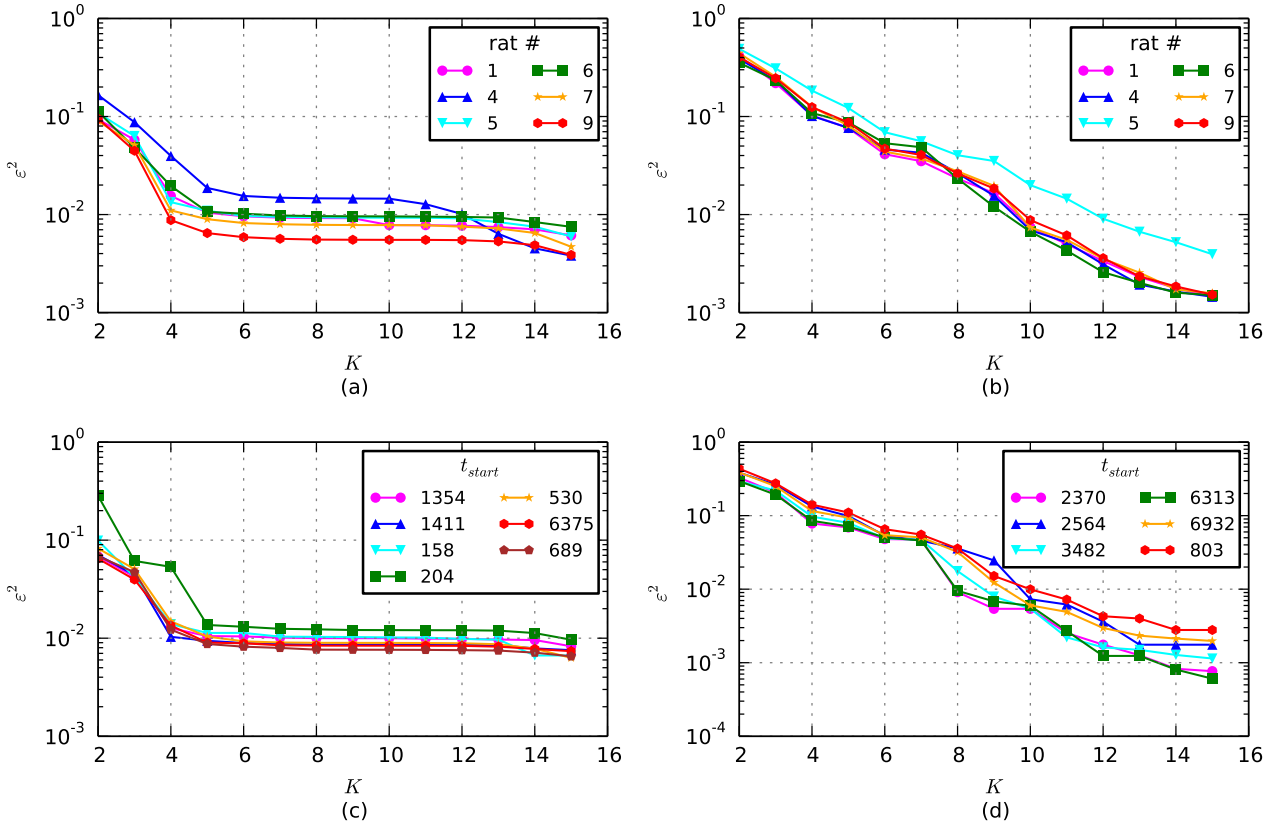

Figure 3. Dependence of the approximation error ε^2 on number of basis functions when constructing a model: (a) — averaged over all seizures per rat error for seizure activity with for different rats; (b) — averaged over all seizures per rat error for baseline activity fragment for different rats; (c) — error for different seizures of the rat #6; (d) — error for different baseline fragments for rat #6. All fragments used were of 2 s length, for seizure fragments $D = 2$, for baseline fragments $D = 5$.

73 absence seizures were detected by visual marking of the cortical layer 6 based on the signal shape and the moving window Fourier analysis. 100% of those seizures were detected using the RBF-model based marking. Sometimes the RBF-based marking divided an SWD into two different parts while the visual marking based on Fourier analysis took it as a single SWD. This may suggest that a long SWD may consist of two shorter SWD.

In average, only about 78(±4)% marks made by the automatic detection method were visually identified SWDs. About 5% of the marks were absence-like signals that resembled pre-seizure signal form, sleep-spindle-like or theta precursors, while approximately 17% of marks appeared to be artefacts.

The mean average deviation of the seizure onset determined using the RBF-based marking tends toward zero compared to the value determined by visual marking. The mean absolute deviation is 0.4 s.

Also the cortical layer 6 of the other five rats was analysed by means of the developed algorithm with at least one set of sample models taken form the studied channel of the rat. Ten SWD onsets were marked visually by an expert for all studied rats. The method detected all SWD onsets marked visually by an expert in each case. After that, sample model sets taken from cortical layer 6 of other five rats were applied to the cortical layer 6 of rat 6. Low-pass and band-pass filters adjustment was performed in all those cases. The results showed that it is possible to attain 100% of the SWD detection using sample models from other rats, but only with about 5% average loss in precision.

Cortical layer 6 has the most pronounced imprint of absence seizures. Nevertheless, analysis of other channels

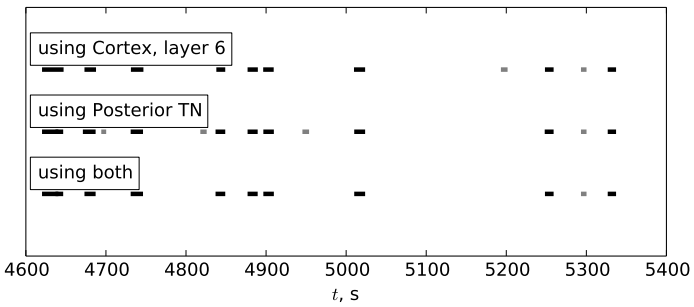

Figure 4. RBF-model based marking example. Correct onsets are pictured in black, false onsets — in grey.

may help to improve accuracy of the method. The reason for most of the artefact detections is that the models which were used to determine absence seizures suit artefacts as good as they suit noisy or blurred absence seizures. However, while absence seizures appear on different channels almost simultaneously, most of the artefacts are channel-specific. Visual marking for the cortical layer 5 is the same as that for cortical layer 6 (with 0.2 s accuracy). The only difference is that the RBF-model based marking results are less precise due to a lower clearness of the signal, as revealed using the Fourier analysis.

The following results were achieved using cortical layer 6 and Posterior thalamus RBF-model based marking. Apart for three transitional segments, 100% absence seizures were detected with 94.8% accuracy. 2 artefacts, 2 absence-like signals and 73 absence seizures occurred in both channels markings simultaneously. Figure 4 illustrates the fact that analysing two channels instead of one may significantly improve the quality of marking.

4. CONCLUSION AND DISCUSSION

A new original method for automatic marking epileptic spike-wave discharges is proposed. The method is based on simultaneous use of two predictive dynamical models exploiting radial basis functions to approximate the dependency of further signal values on the set of previous ones. One model is constructed from a fragment *a priori* recognised as a seizure and the other — from a segment recognised as a baseline. The low-pass filter for the maximum suitable error value of a seizure model and the band-filter for the suitable error values of a baseline model were set manually. Then these two models were applied as a scanner with a moving window, automatically marking seizure onsets and offsets.

The following method advantages can be mentioned:

1. The method revealed a good temporal resolution, because its temporal accuracy determined by a model length (summary time delay for state vector reconstruction plus prediction time) is usually short (significantly less than 1 s for the considered cases).

2. The method is precise, since its mean error while recognising seizure onsets is close to zero, and its standard error of the mean is ≈ 0.4 s.

3. The method can be applied in real time since the most time-consuming calculation step — a construction of two predictive models — is performed off line, only once for each subject.

4. The method is robust for individual specifics of data. Models based on well-pronounced absences of other rats gave only about 5% more false alarms then models based on the studied rat absences, with the same 100% amount of detected absences. Moreover, the optimal model parameters do not differ for different seizures and different subjects.

5. The method is highly automatic: the only real tuning for the new data needed is predefining one baseline and one absence fragments for model fitting, then setting boundaries of the low-pass filter for an absence model error and of a band-pass filter for a baseline model error.

The method showed relatively high accuracy, especially when two channels, one from the cortex and the other one from the thalamus were used, so it can benefit from multichannel data: accuracy grew from 78% for the best one single channel to 94.8% for two channels. In addition, the accuracy may be increased further if more channels are included into the procedure.

5. ACKNOWLEDGEMENTS

This research was funded by Russian Scientific Foundation, Grant No. 14-12-00291.

REFERENCES

[1] Sander, J. W., "The epidemiology of epilepsy revisited," *Current Opinion in Neurology* **16**, 165–170 (2003).

[2] Fisher, R. S., van Emde Boas, W., Blume, W., Elger, C., Genton, P., Lee, P., and Engel, J., "Epileptic seizures and epilepsy: Definitions proposed by the international league against epilepsy (ilae) and the international bureau for epilepsy (ibe)," *Epilepsia* **46 (4)**, 470–472 (1999).

[3] McNamara, J. O., "Emerging insights into the genesis of epilepsy," *Nature* **399**, 15–22 (1999).

[4] Fell, J. and Axmacher, N., "The role of phase synchronization in memory processes," *Nature Reviews Neuroscience* **12 (2)**, 105–118 (2011).

[5] Panayiotopoulos, C. P., "Treatment of typical absence seizures and related epileptic syndromes," *Paediatric Drugs* **3**, 379–403 (2001).

[6] Whisler, J. W., Remine, W. J., Leppik, I. E., McLain, L. W. J., and Gumnit, R. J., "Machine detection of spike-wave activity in the eeg and its accuracy compared with visual interpretation," *Electroencephalography and clinical Neurophysiology* **54**, 541–551 (1982).

[7] van Luijtelaar, G., Sitnikova, E., and Lüttjohann, A., "On the origin and suddenness of absences in genetic absence models," *Clin EEG Neurosci* **42 (2)**, 83–97 (2011).

[8] Lüders, H. and Noachtar, S., [*Atlas of Epileptic Seizures and Syndromes*], Elsevier Science Health Science Division (2001).

[9] Sartorettoa, F. and Ermanib, M., "Automatic detection of epileptiform activity by single-level wavelet analysis," *Clinical Neurophysiology* **110**, 239–249 (1999).

[10] Ovchinnikov, A., Lüttjohann, A., Hramov, A., and van Luijtelaar, G., "An algorithm for real-time detection of spike-wave discharges in rodents," *J. of Neuroscience Methods* **194 (1)**, 172–8 (2010).

[11] Kalayci, T. and Özdamar, Ö., "Wavelet preprocessing for automated neural network detection of eeg spikes," *IEEE Engineering in Medicine and Biology* **14 (2)**, 160–166 (1995).

[12] Buteneers, P., Verstraeten, D., Nieuwenhuyse, B. V., Stroobandt, D., Raedt, R., Vonck, K., Boon, P., and Schrauwen, B., "Real-time detection of epileptic seizures in animal models using reservoir computing," *Epilepsy Research* **103**, 124–134 (2013).

[13] Bezruchko, B. and Smirnov, D., [*Extracting Knowledge From Time Series*], Springer (2010).

[14] Buhmann, M. D., [*Radial Basis Functions: Theory and Implementations (Cambridge Monographs on Applied and Computational Mathematics)*], Cambridge University Press (2003).

[15] Ancona, N., Marinazzo, D., and Stramaglia, S., "Radial basis function approach to nonlinear granger causality of time series," *Physical Review E* **70**, 056221 (2004).

[16] Marinazzo, D., Pellicoro, M., and Stramaglia, S., "Nonlinear parametric model for granger causality of time series," *Physical Review E* **73**, 066216 (2004).

[17] Tan, P. N., Steinbach, M., and Kumar, V., [*Introduction to Data Mining*], Addison-Wesley (2005).

[18] Schwarz, G., "Estimating the dimension of a model. annals of statistics," *Annals of Statistics* **6 (2)**, 461–464 (1978).

[19] McQuarrie, A. D. R. and Tsai, C. L., [*Regression and time series model selection*], World Scientific (1998).

[20] Lüttjohann, A. and van Luijtelaar, G., "The dynamics of cortico-thalamo-cortical interactions at the transition from pre-ictal to ictal LFPs in absence epilepsy," *Neurobiology of Disease* **47**, 47–60 (2012).

[21] Paxinos, G. and Watson, C., [*The Rat Brain in Stereotaxic Coordinates, 6th Edition*], San Diego: Academic Press (2006).